Journal of Molecular Catalysis A: Chemical 287 (2008) 151–158

Contents lists available at ScienceDirect

Journal of Molecular Catalysis A: Chemical

journal homepage: www.elsevier.com/locate/molcata

Visible light induced photocatalytic activity of rare earth titania nanocomposites

K.M. Parida*, Nruparaj Sahu

Colloids and Materials Chemistry Department, Institute of Minerals and Materials Technology (CSIR), Bhubaneswar 751013, Orissa, India

ARTICLE INFO

Article history:
Received 28 December 2007
Received in revised form 22 February 2008
Accepted 25 February 2008
Available online 8 March 2008

Keywords:
Rare earth metal oxides
Hexavalent chromium
Methylene blue

ABSTRACT

Rare earth metal oxides doped TiO_2 were prepared by an incipient wetness impregnation method by varying different mol% of La, Nd and Pr and characterized by various advanced techniques such as powder X-ray diffraction (PXRD), BET-surface area, N_2 adsorption–desorption measurements, UV–vis DRS, FTIR and scanning electron microscope (SEM). Analytical results demonstrated that the TiO_2 nanoparticles are mesoporous in nature and doping of lanthanides could inhibit the phase transformation, increases the surface area and decreases the crystallite size of mesoporous structures of TiO_2. We investigated the visible light induced photocatalytic activities of these materials towards reduction of hexavalent chromium and degradation of methylene blue for the first time. La^{3+}-TiO_2 containing 0.4 mol% lanthanum, activated at 673 K showed highest surface area (124.8 m^2/g), lowest crystallite size (8 nm) and exhibits highest photocatalytic activity. The reduction of hexavalent chromium and methylene blue degradation rate followed first-order kinetics.

1. Introduction

The study of light-induced reactions catalyzed by semiconductors such as TiO_2 [1,2], ZnO [3], CdS, ZnS, WO_3 [4], etc., has been widely studied during the past decade. TiO_2 is one of the most important semiconducting oxides because of its photocatalytic activity, conservative nature, low cost, low toxicity, and stable to light illumination. Other than these properties, its eminent capability of photocatalytic decomposition of organic materials has come to utilization in the environmental business, i.e., organic pollutant treatment [5,6]. However TiO_2 has high band gap energy (3.2 eV), which limits its wide application in visible light range of solar spectrum. A good photocatalyst depends strongly on its efficiency of electron–hole pair separation and its optical absorption property. To effectively eliminate the electron–hole recombination in the photocatalytic reaction, titania has been modified by doping with impurities such as various transition metals, inner transition metals [7–13], sulphate [14], etc. Metal ion doping has been proven to be an efficient root to alter both the photoactivity and anatase–rutile phase transformation of TiO_2. The suitable metal ion doping appears to be the most important factor in the enhancement of photoreactivity of doped TiO_2. Recently, doping lanthanide into TiO_2 has attracted much attention [15–18]. Lanthanide ions are known for their ability to form complexes with various Lewis bases (e.g., amines, aldehydes, alcohols, thiols, etc.) in the interaction of these functional groups with the f-orbital of the lanthanides. Thus, incorporation of lanthanide ions into a TiO_2 matrix could provide a means for concentration of the organic pollutant at the semiconductor surface and there fore enhances the photocatalytic activity of the catalyst [19–21].

Out of the total world production of dyes, 15% is lost during the dying process and is released in textile effluents [22,23]. These effluents contain azo dyes and huge amount of inorganic salts. Physical methods such as adsoption, biological methods and chemical methods are the most frequently used for the treatment of these textile dyes. Among the textile dyes methylene blue (MB) is a brightly coloured blue cationic thiazine dye with λ_{max} at 665, 614, 292 nm. Chromium exhibits variable oxidation states, out of which Cr (VI) and Cr (III) are common. Cr (VI) is mobile and highly toxic where as Cr (III) is mostly immobile and less harmful. The major source of Cr (VI) is improper discharge of various industrial wastewaters. Among them potential sources are pigments, photographic materials, dyes, plastics, inks, stainless steel production, textile dyes, wood preservation, leather tanning, cement industries, mining, etc. The methods employed for the removal of Cr (VI) are chemical precipitation, chromatography, foam flotation, electrolysis, reverse osmosis, photocatalytic reduction, adsorption, etc.

* Corresponding author. Tel.: +91 674 2581636 425; fax: +91 674 2581637.
E-mail address: kmparida@yahoo.com (K.M. Parida).

1381-1169/$ – see front matter © 2008 Elsevier B.V. All rights reserved.
doi:10.1016/j.molcata.2008.02.028

However, most of the methods require either high energy or large quantities of chemicals where as photocatalytic process is found to be superior to all.

The present study deals with the textural characterization and visible light induced photocatalytic activity of rare earth (La, Pr and Nd) titania nanocomposites towards reduction of hexavalent chromium and degradation of methylene blue.

2. Experimental

2.1. Material preparation

Hydrated titania was prepared by sol–gel method, taking tetraisopropyl orthotitanate (Fluka, Chemica 98%) as starting material. In a typical preparation procedure, 50 ml of tetraisopropyl orthotitanate was dissolved in 400 ml of isopropanol (Qualigens 99.7%) and to this solution 12.7 ml of distilled water at pH 3.0 (1 M HNO_3) was added drop wise under vigorous stirring. The resulting colloidal suspension was stirred for 3 h and aged at 353 K for 10 h. The gel obtained was filtered, washed and dried at 373 K for 12 h.

Rare earth (La, Pr and Nd) doped titania samples with varying the mol% (0.2, 0.4, 0.6 and 0.8) of rare earth were prepared by an incipient wetness impregnation method taking rare earth nitrates. The prepared samples were calcined at 673, 773, 873, 973 and 1000 K at the heating rate of 10 K/min in a muffle furnace four 4 h.

2.2. Physico-chemical characterization

In order to determine the crystal phase composition of the catalyst, powder X-ray diffraction (PXRD) was carried out on Philips X-ray diffractometer (PW 3710, Co anode). Specific surface area (BET) of the catalysts was measured by N_2 adsorption–desorption studies at liquid nitrogen temperature (77 K) using Quantasorb (Quantachrome, USA). Prior to the analysis, samples were degassed at 473 K. UV–vis DRS spectra was recorded in UV–vis Spectrometer (Shimadzu). The spectra were recorded in the range of 200–800 nm using boric acid as the reference standard. Surface morphology and particle size were studied by scanning electron microscope (SEM) (Hitachi S-3400N). The specimen for SEM analysis was prepared by gold sputtering process. FTIR spectra of the samples were recorded in a Varian FTIR spectrophotometer (FTS-800) in the range of 400–4000 cm^{-1} taking KBr as the reference.

2.3. Photocatalytic activity

The photocatalytic reduction of hexavalent chromium and degradation of MB was conducted separately. The photocatalytic reduction of hexavalent chromium was performed with 25 ml of 20 mg/l Cr (VI) solution ($K_2Cr_2O_7$, BDH, India) and degradation of MB was carried out by taking 20 ml of 100 mg/l methylene blue (s.d.fine-chem Ltd., Mumbai) solution in a 100 ml closed Pyrex flask, over 1.0 g/l of catalyst. The pH of the dispersion was adjusted with dilute solution of sulphuric acid (BDH). The solutions were exposed to sunlight at room temperature with constant stirring. All the irradiations were performed in triplicate during the March 2006 (sunny days), from 10.00 a.m. to 14.00 p.m. when the average solar intensity was 0.80 kW/m^2 and the intensity fluctuations were minimal. Reactions were performed in the dark in order to determine the adsorption behavior of the catalysts under similar conditions. Blank experiment was performed to know the extent of photoreaction due to solar radiation. After irradiation, the suspension was centrifuged. Then Cr (VI) content was analyzed quantitatively at 348 nm and the methylene blue content was analyzed quantitatively at 660 nm using Cary-1E (Varian, Australia) spectrophotometer. All the experimental results were reproducible with ±4% variation.

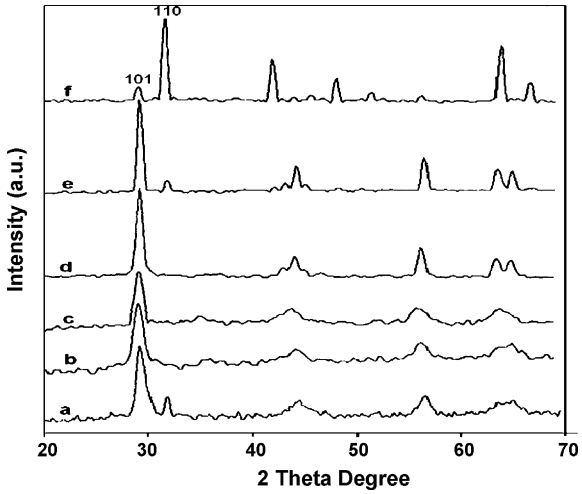

Fig. 1. PXRD pattern of (a) TiO_2 activated at 673 K, 0.4 mol% La doped titania activated at (b) 673 K, (c) 773 K, (d) 873 K, (e) 973 K, and (f) 1073 K.

3. Results and discussion

3.1. Physico-chemical characterization

The PXRD patterns of rare earths (La^{3+}, Pr^{3+}, Nd^{3+}) doped TiO_2 (calcined at 773 K) are similar, containing only anatase phase (figure not shown). The X-ray diffraction patterns of the pure TiO_2 and La^{3+} doped TiO_2 samples activated at different temperatures are shown in Fig. 1. From PXRD pattern, the percentage of anatase phase can be calculated by Eq. (1).

$$\%\ \text{of anatase phase} = \frac{100}{1 + I_R/0.79I_A} \quad (1)$$

where I_A and I_R is the intensity of strongest diffraction line (1 0 1) of anatase phase and (1 1 0) of rutile phase, respectively (Eq. (1)) [9].

The crystallite sizes (D) of anatase and rutile phase of samples were determined by employing Debye–Scherrer formula (Eq. (2)) and listed in Table 1.

$$D = K\lambda/\beta\cos\theta \quad (2)$$

where λ is wavelength of the Co Kα used, β is the full width at half maximum of the diffraction angle considered, K is a shape factor (0.94) and θ is the angle of diffraction. The peaks (1 0 1) for anatase and (1 1 0) for rutile were used.

PXRD pattern shows that both anatase and rutile phases are present in pure TiO_2, activated at 673 K. But in case of La^{3+} doped TiO_2 calcined at the same temperature, only anatase phase is present. From this result, we believed that La^{3+} doping probably inhibits the phase transformation. However, the phase transformation took place at higher temperature. Small fraction of rutile phase appears for the sample activated at 973 K, whereas in case sample calcined at 1073 K, it is dominated by rutile phase. The crystallite size of TiO_2 in La^{3+}-TiO_2 samples increases with increasing the activation temperature (Table 1). However, crystallite size of pure TiO_2 is greater than La^{3+}-TiO_2, activated at the same temperature. This may possibly be due the fact that the La^{3+} doping of TiO_2 could stabilize the crystallite size.

The N_2 adsorption–desorption isotherms and the pore size distribution of TiO_2 and 0.4 mol% La^{3+}-TiO_2 samples are shown in Fig. 2(a) and (b), respectively. Type IV isotherm and H1 hysteresis loop was observed which clearly indicates the mesoporous

Table 1
Crystallite size, *d*-spacing and lattice parameter of neat and La^{3+} doped titania

Photocatalysts	Crystal composition	Crystal size (nm)	d_{101}/d_{110} (nm)	*a* (nm)	*c* (nm)
TiO_2 (673 K)	Anatase (81%)	9.79	3.51	0.37774	0.94992
	Rutile (19%)	–	3.29	–	–
0.4 mol% La^{3+}-TiO_2 (673 K)	Anatase only	8.91	3.52	0.37772	0.94756
0.4 mol% La^{3+}-TiO_2 (773 K)	Anatase only	13.5	3.52	0.37772	0.94976
0.4 mol% La^{3+}-TiO_2 (873 K)	Anatase only	14.63	3.52	0.37808	0.95276
0.4 mol% La^{3+}-TiO_2 (973 K)	Anatase (87%)	17.07	3.51	0.37854	0.95164
	Rutile (13%)	–	3.25	–	–
0.4 mol% La^{3+}-TiO_2 (1073 K)	Anatase (8%)	–	3.53	–	–
	Rutile (92%)	17.24	3.27	0.44973	0.29925

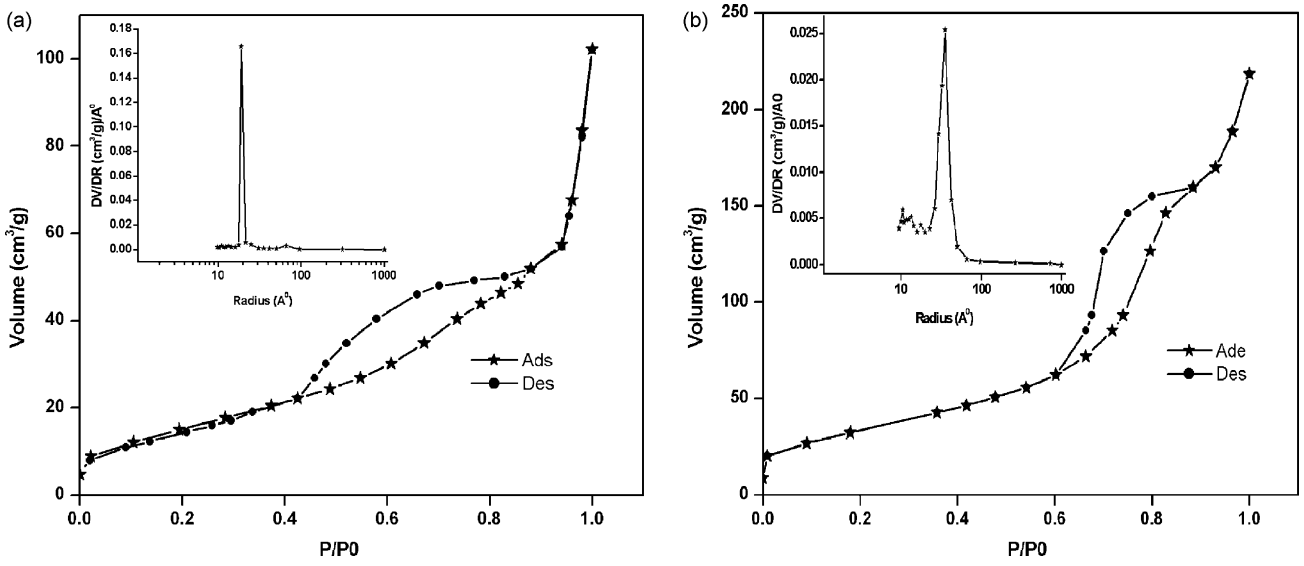

Fig. 2. N_2 adsorption–desorption isotherm and pore size distribution of 673 K activated (a) TiO_2 and (b) 0.4 mol% La/TiO_2.

nature of TiO_2. Pore volume (single point total pore volume of pores at $P/P_o = 0.99$) and pore size (determined from BJH desorption isotherm) of the samples are given in Table 2. On increasing the activation temperature of the catalyst, pore volume decreases and pore size increases. This may be due to the collapse of mesoporous structure upon calcinations, which results in the shifting of pore size to a larger mesoporous region.

The BET specific surface areas of rare earth doped samples calcined at 673 K were in the range of 104–125 m^2/g. When we compare the results with the undoped samples, the relative high surface area of doped samples confirms that the frameworks of mesoporous TiO_2 have better thermal stability. This may be due to the formation of rare earth titania composites oxides, which effectively enhancing surface area of TiO_2.

The UV–vis DRS spectra of pure and La^{3+} doped TiO_2 is shown in Fig. 3. It was observed that the absorption edges of La^{3+} doped TiO_2 shift slightly towards longer wavelength (red shift) compare to that of pure TiO_2, for which the samples were active under visible light of the solar spectrum.

The FTIR spectra of pure TiO_2 and 0.4 mol% La^{3+}-TiO_2, calcined at 673 K are shown in Fig. 4. It is believed that the broad absorption band in the region of 3200–3400 cm^{-1} is characteristic of OH- stretching vibration of surface hydroxyl group and peak cor-

Table 2
Surface property of neat and La^{3+} doped titania

Photocatalysts	S_{BET} (m^2/g)	Pore volume (cm^3/g)	Pore size (nm) (average pore radius)
TiO_2 as synthesized	625.7	0.58	2.06
TiO_2 (673 K)	59.2	0.13	3.59
0.4 mol% La^{3+}-TiO_2 (673 K)	124.8	0.44	6.5
0.4 mol% La^{3+}-TiO_2 (873 K)	33.3	0.20	10.6
0.4 mol% La^{3+}-TiO_2 (1073 K)	17.0	0.08	23.7

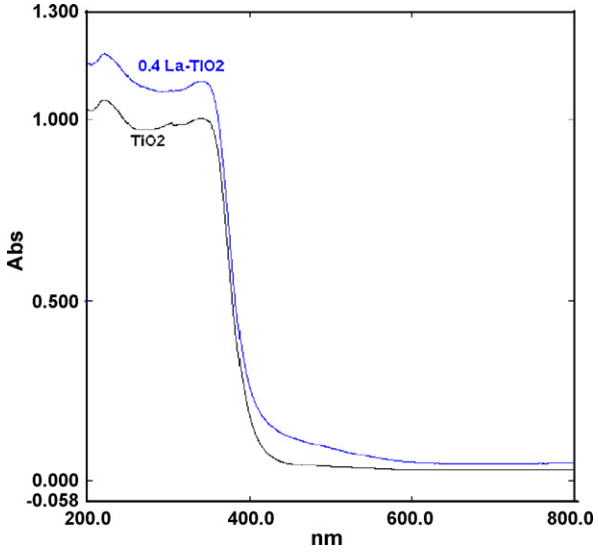

Fig. 3. UV–vis DRS spectra of neat and La^{3+} doped TiO_2.

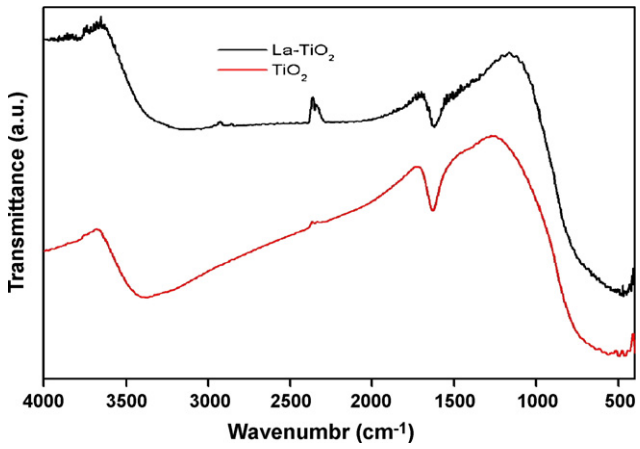

Fig. 4. FTIR spectra of 673 K activated (a) TiO_2 and (b) 0.4 mol% La/TiO_2.

responding to 1620 cm^{-1} has been assigned to H—O—H bending of physically adsorbed water. The peaks at 436 and 495 cm^{-1} for pure TiO_2 and 476 cm^{-1} for 0.4 mol% La^{3+}-TiO_2 are due to the vibration modes of anatase skeletal O—Ti—O and O—Ti—O—La bonds [24–26], which is also supported by PXRD (Fig. 1).

SEM micrographs of undoped TiO_2 and 0.4 mol% La^{3+}-TiO_2 are shown in Fig. 5(a). The particles were found to be in spherical shape. Undoped TiO_2 particles were found to be in the form of aggregation unlike La^{3+} doped TiO_2. La^{3+} ion modification preferably retarded the aggregation and growth of well-dispersed particles. The La^{3+} ion existed in the wall of the obtained samples is confirmed by energy dispersive X-ray spectroscopy (EDX) measurement (Fig. 5(c)) and the concentration of Ti and La elements in the selected area is shown in X-ray image mapping of the sample (Fig. 5(b)).

3.2. Photocatalytic activity

3.2.1. Photocatalytic degradation and dark adsorption

It was observed that in absence of catalyst, the photoreduction of Cr (VI) is very negligible (only 2.0%) and degradation of MB is only 5.0% after 4 h irradiation under solar radiation. It was found that 86.5% of Cr (VI) reduction and 80.0% of MB degradation takes place by taking 20 mg/L Cr (VI) solution and 100 mg/l MB solution over 1.0 g/l of 0.4 mol% La^{3+}-TiO_2 catalyst, under solar radiation. Where as 17% of adsorption takes place under similar conditions in dark. The equilibrium is achieved in 4 h of illumination.

3.2.2. Effect of lanthanides

In order to evaluate the photocatalytic activity of Ln^{3+}-TiO_2, a set of Cr (VI) reduction and MB degradation test was carried out by varying dopant content (0.2, 0.4, 0.6, 0.8 mol%) in Ln^{3+}-TiO_2 (Fig. 6(a) and (b)). It was demonstrated that all the TiO_2 catalysts doped with Ln^{3+} increases the percentage of reduction/degradation (in case of pure TiO_2 45% of Cr (VI) reduction and 30% of MB degradation where as after La^{3+} doping 86% of Cr (VI) reduction and 80% of MB degradation was observed). Not much difference was observed among different lanthanides, i.e., La^{3+}-, Nd^{3+}-, Pr^{3+}-TiO_2 catalysts towards the reduction of Cr (VI) or degradation of MB. Moreover it was observed that TiO_2 catalyst containing 0.4 mol% La^{3+} shows higher catalytic activity under solar radiation (around 86.5 of Cr (VI) reduction and 80% of MB degradation), which would be the optimum dose of lanthanum doping for forming nanocomposite of rare earth and titania oxide.

The crystalline phase of the titania is an important factor that determines its activity. Previous reports have indicated that the rutile phase is less active in the photodegradation of organic compounds [27,28]. The lanthanide oxide-containing catalysts exist in the anatase phase whereas the non-modified TiO_2 catalyst contains rutile phase (ca. 20%). However the significant differences obtained in the photocatalytic activities cannot be attributed to the differences in the phase composition. Another factor that could influence significantly the photocatalytic activity is the surface area of the catalysts. The surface areas of Ln^{3+}/TiO_2 are 124 m^2/g while that of the unmodified TiO_2 is only 59 m^2/g. Along with surface area, the electronic structure and surface properties such as space charge layer, surface states, and their concentration are important parameters that are affected by doping of a semiconductor with altervalent ions [19]. Thus doping of TiO_2 semiconductor with lower valent ions such as Ln^{3+} increases the work function; hence, the Fermi energy level is shifted to lower values. Consequently, on contact with an electrolyte, the depletion layer of the p-doped semiconductor becomes thicker as compared to the non-modified semiconductor. As a result, the capacity of the space charge region to separate the electron–hole pair is reduced [29]. Modification of the surface state of the catalyst might be causing effective separation of electron–hole pairs (e^-h^+).

In fact the ionic radius of La^{3+} (0.115 nm) is bigger than that of Ti^{4+} (0.068 nm). Therefore, it is difficult for La^{3+} to really enter into the lattice of TiO_2. However, there is slight difference in the lattice parameters "*a*" and "*c*" between pure TiO_2 and La^{3+}-TiO_2. It might be due to the substitution of La^{3+} atoms in the lattice of La_2O_3 by Ti^{4+}. A Ti—O—La bond could be formed at the interface. If Ti^{4+} replace La^{3+}, a charge imbalance would occur. Therefore, both formation of Ti—O—La bond and charge imbalance might affect the photocatalytic activity of La^{3+}-TiO_2 catalyst [13]. The charge imbalance must be satiated, so more hydroxide ions would be adsorbed onto the surface for charge balance. These hydroxide ions on the surface can accept holes generated by light irradiation to form hydroxyl radicals, which oxidize adsorbed substrates. Therefore, the photoinduced charge carriers recombination can be suppressed. Xu et al. [30] reported that when the concentration of dopant ions increases, the surface barrier becomes higher, and the space charge region becomes narrower, the electron–hole pairs within the region are efficiently separated by the large electric field before recombination. On the other hand, when the concentration of doping ions is high, the space charge region becomes very narrow and the penetration depth of light into TiO_2 greatly exceeds the space charge layer; therefore the recombination of the photogenerated electron–hole pairs in semiconductor become easier. Consequently, there is an optimum concentration of dopant ions to make the thickness of space charge layer substantially equal to the light penetration depth. Excess amounts of rare earth oxide covering the surface of TiO_2 would increase the number of recombination centers and result in low photoactivity. So it is not a surprise that the mixed TiO_2-rare earth oxides with more than 0.4 wt% rare earth show less photocatalytic activity. However in the present investigation we have found that the activity of the lanthanide oxide-doped TiO_2 semiconductor is significantly higher than the non-modified TiO_2 semiconductor. This would suggest that the equilibrium dark adsorption of the pollutant at the photocatalyst surface have an important role in determining the photocatalytic activity. The adsorption was found to be higher on the lanthanide oxide-modified catalysts as compared to the non-modified catalysts. This can be attributed to the formation of Lewis acid–base complexes between the lanthanide ions and MB.

3.2.3. Effect of pH

Photocatalytic reduction of hexavalent chromium and degradation of MB is pH dependent. At lower pH (pH ~ 2–3), percentage

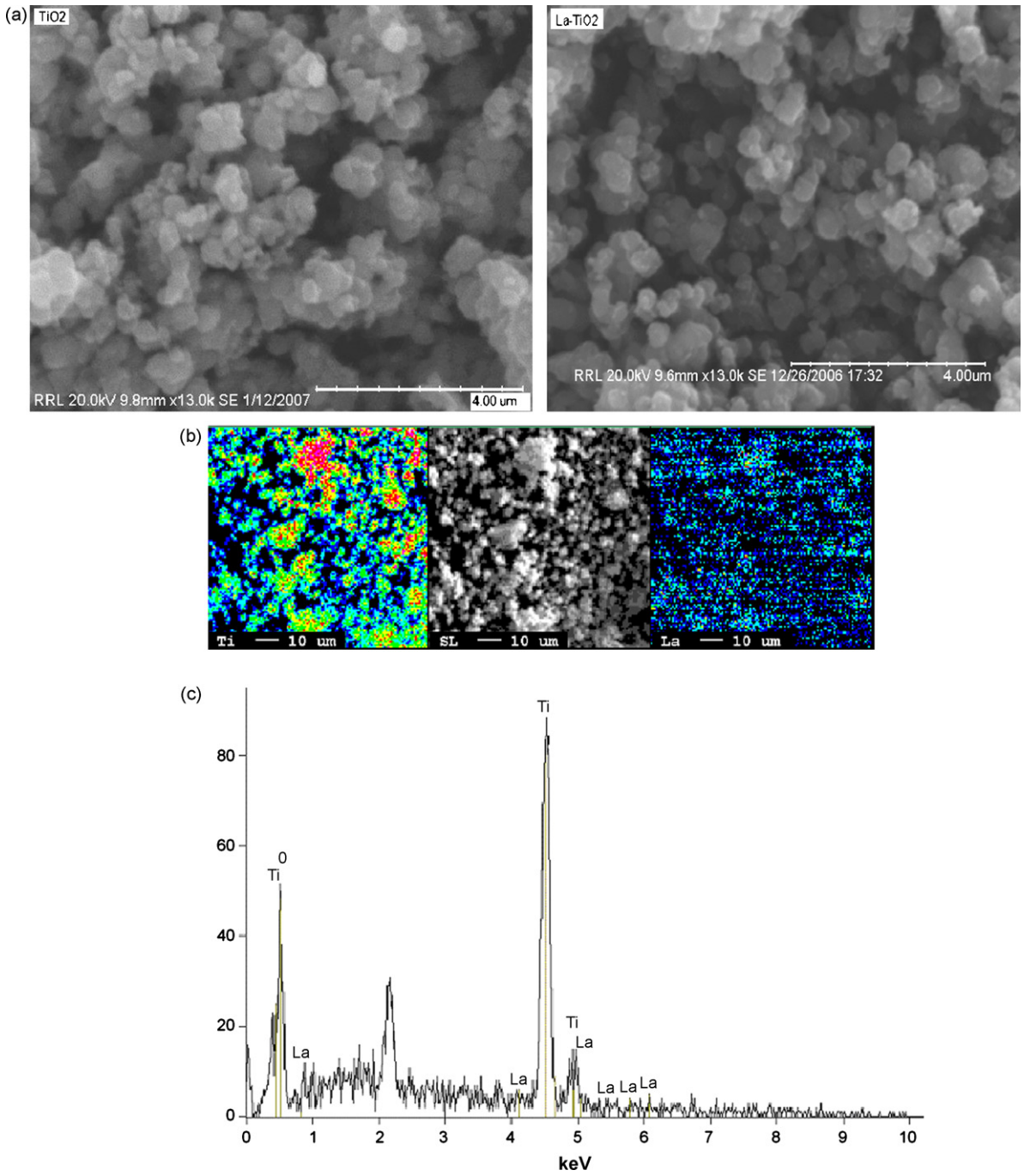

Fig. 5. (a) SEM micrographs of 673 K activated TiO_2 and 0.4 mol% La/TiO_2. (b) X-ray image mapping of 0.4 mol% La/TiO_2 activated at 673 K. (c) EDX spectrum of La/TiO_2 sample.

of photoreduction is maximum (around 94%) and it gradually decreases with increase in pH (Fig. 7(a)). The photocatalytic degradation of MB is favoured at higher pH (Fig. 7(b)). This can be explained on the basis of point of zero charge (pH_{pzc}). Point of zero charge (pH_{pzc}) of the catalyst (0.4 mol% La^{3+}-TiO_2) was found to be 5.3–5.7. It can be assumed that for pH lower than the pH_{pzc}, the positive excess charge at the catalyst surface due to the surface adsorption of H^+ ions favours the approach of anionic Cr (VI) species to the catalyst surface, where as for higher pH excess of adsorbed OH^- ions has the opposite effect, leading to low level of adsorbed Cr (VI). In case of MB opposite effect was found, as it is a cationic dye.

3.2.4. Effect of activation temperature of photocatalyst

On increasing the activation temperature of the catalyst from 673 to 1073 K, the percentage of reduction/degradation decreases from 86.5 to 62% for Cr (VI) (Fig. 8(a)) and 80 to 52% for MB (Fig. 8(b)). However there is increase in the percentage of reduction/degradation in case of catalyst activated at 973 K, which may be due to the synergetic effect of anatase and rutile phase. On further increase in temperature, the percentage of reduction//degradation decreases. This may be due to the decrease in surface area (from 124.8 to 17.0 m^2/g), pore volume (0.44–0.08 cm^3/g) of the catalyst.

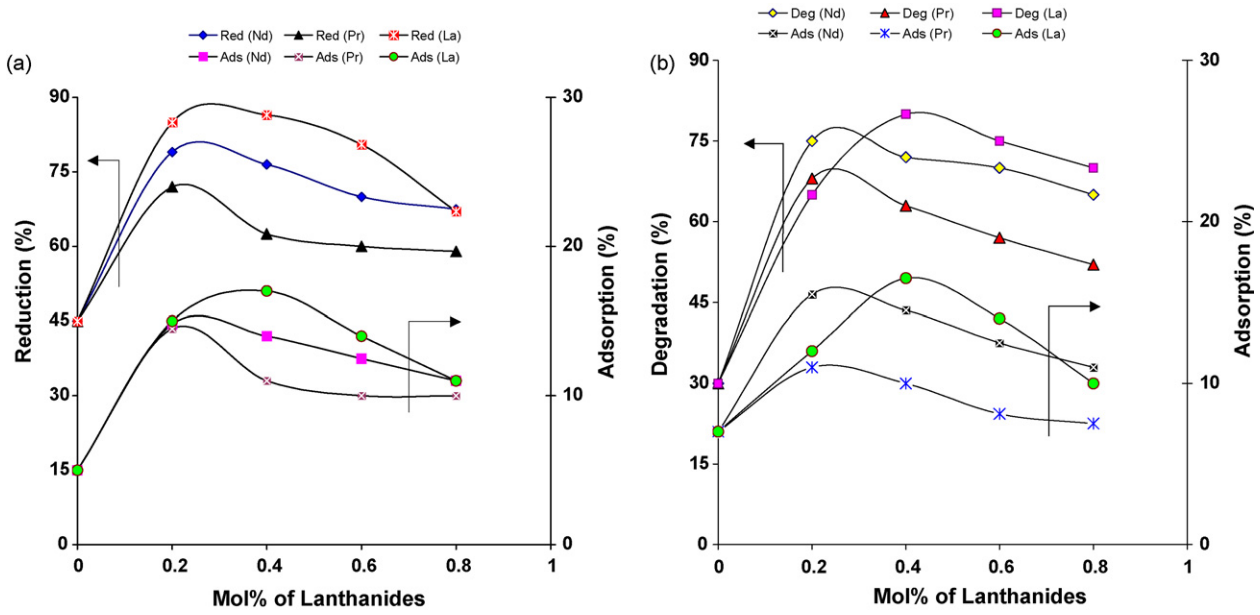

Fig. 6. (a) Effect of lanthanides on the photo reduction and dark adsorption of Cr (VI): catalyst dose = 1.0 g/l; [Cr (VI)] = 20 mg/l; time = 4 h. (b) Effect of lanthanides on the photodegradation and dark adsorption of MB: catalyst dose = 1.0 g/l; [MB] = 100 mg/l; time = 4 h.

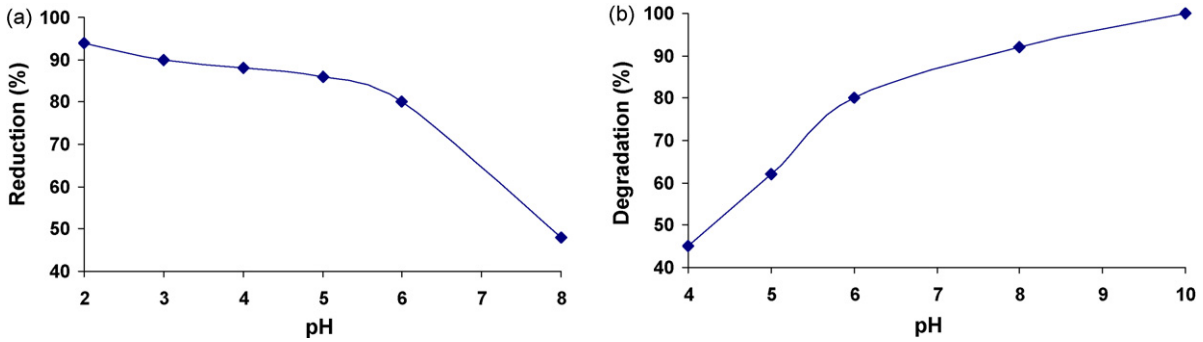

Fig. 7. (a) Effect of pH on the Cr (VI) photo-reduction: catalyst dose = 1.0 g/l; [Cr (VI)] = 20 mg/l, time = 4 h. (b) Effect of pH on MB degradation: catalyst dose = 1.0 g/l; [MB] = 100 mg/l; time = 4 h.

3.2.5. Kinetics

A linear relationship was observed between the concentration and irradiation time. The plot of $\log(C_o/C)$ versus time, where C_o is the initial concentration and C is the concentration at any time t as shown in Fig. 9(a) and (b) for the photoreduction of Cr (VI) and degradation of MB, respectively. This indicates that photoreduction of Cr (VI) and degradation of MB follows first-order kinetics. The calculated data for first-order rate constants "k" at 10 and 20 ppm Cr (VI) concentration were found to be 0.816 and 0.60 h^{-1} where as for 50 and 100 ppm MB concentration it was found to be 1.65 and 0.466 h^{-1}. The rate constant values were found to decrease with increase in initial concentration of Cr (VI) and MB.

3.2.6. Mechanism

During photocatalysis, adsorption of Cr (VI) occurred first when TiO_2 was dispersed in the aqueous solution containing hexavalent chromium. The reduction of Cr (VI) to Cr (III) occurs because under

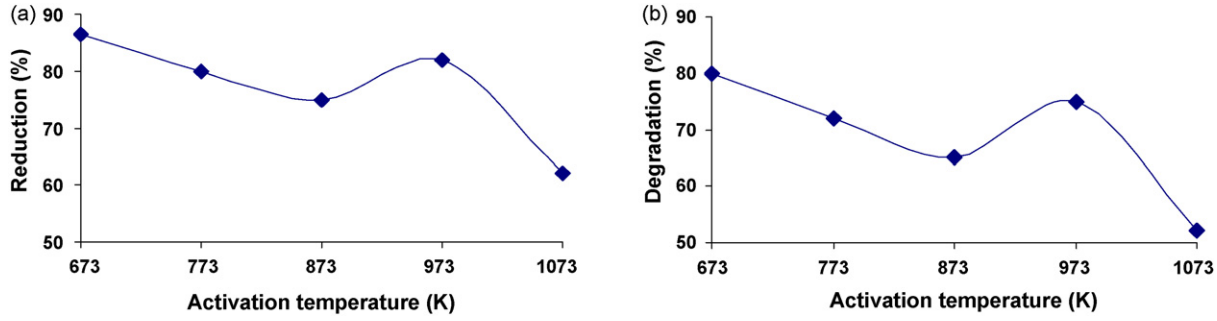

Fig. 8. (a) Effect of activation temperature of the catalyst on Cr (VI) photo-reduction: catalyst dose = 1.0 g/l; [Cr (VI)] = 20 mg/l; time = 4 h. (b) Effect of activation temperature of the catalyst on MB degradation: catalyst dose = 1.0 g/l; [MB] = 100 mg/l; time = 4 h.

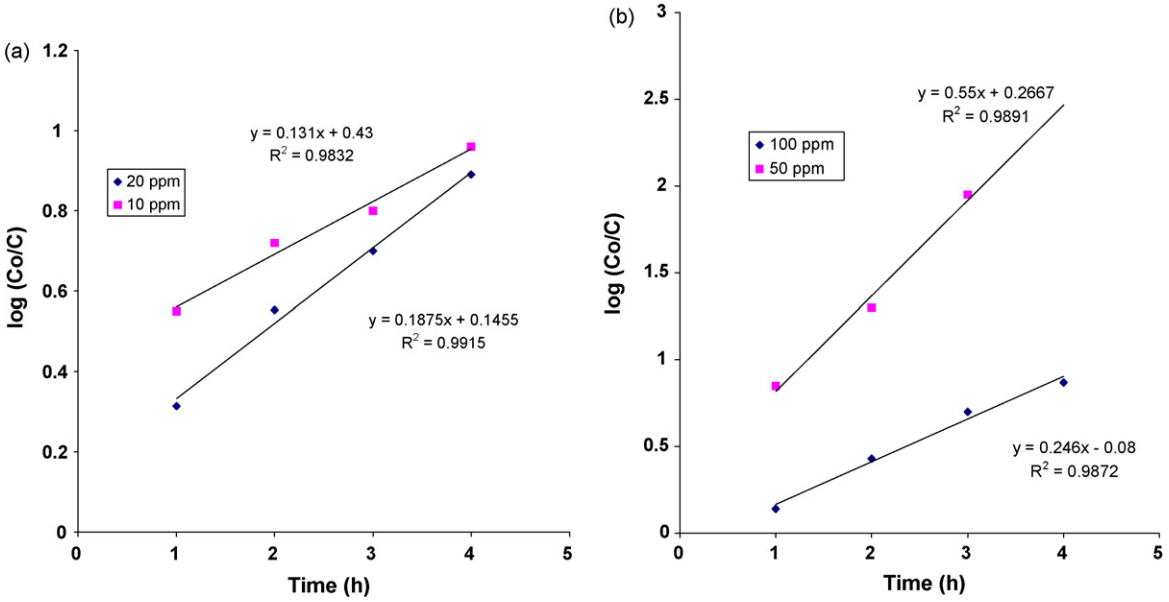

Fig. 9. Kinetics of (a) reduction of Cr (VI) and (b) degradation of MB: catalyst dose = 1.0 g/l; [Cr (VI)] = 20 mg/l; [MB] = 100 mg/l.

illumination electron–hole pairs are created inside the semiconductor particles. After migration of these species to the surface of the semiconductor, the photogenerated electrons reduce Cr (VI) to Cr (III) and holes oxidize water. The possible mechanism of the photocatalytic reduction of hexavalent chromium is as follows:

$$TiO_2 \rightarrow h_{vb}^{+} + e_{cb}^{-}$$

$$Cr_2O_7^{2-} + H^+ + e_{cb}^{-} \rightarrow Cr^{3+} + H_2O$$

$$H_2O + h_{vb}^{+} \rightarrow OH^{\bullet} + H^+$$

This is also supported by Munoz and Doménech [2].

When photocatalytic oxidation is conducted in aqueous medium, the holes were effectively scavenged by the water and generated hydroxyl radicals $OH^{\bullet}$, which are strong and unselected oxidant species in favour of totally oxidative degradation for organic substrates. Both holes and hydroxyl radicals have been proposed as the oxidizing species responsible for the degradation of the organic substrates [31–33].

$$TiO_2 + hv \rightarrow h_{vb}^{+} + e_{cb}^{-}$$

$$h_{vb}^{+} + H_2O \rightarrow OH^{\bullet} + H^+$$

$$h_{vb}^{+} + \text{dye} \rightarrow \text{products}$$

$$OH^{\bullet} + \text{dye} \rightarrow \text{products}$$

$$MB + TiO_2 \xrightarrow{hv} CO_2 + H_2O + NO_3 + NH_4^+ + SO_4^{2-}$$

4. Conclusions

The photocatalytic activity of rare earth oxide doped titania towards the reduction of Cr (VI) and degradation of MB is enhanced may be due to the formation of nanocomposites. This is probably due to availability of higher adsorption sites, red shifts, increase the BET surface area, decrease the crystallite size and prevention of electron–hole recombination. The loading of the lanthanide ions is also an important parameter. Ln^{3+}-TiO_2 containing 0.4 mol% lanthanum, exhibits highest photocatalytic activity. It was observed that reduction of Cr (VI) to Cr (III) takes place at acidic condition and degradation of MB favors under basic condition. The reduction of hexavalent chromium and MB degradation rate followed first-order kinetics.

Acknowledgements

The support and permission of Prof. B.K. Mishra, Director, Institute of Minerals and Materials Technology (CSIR), Bhubaneswar is greatly acknowledged. Authors are very much thankful to Dr. (Mrs.) S. Anand, H&EM Department for PXRD analyses. We are very much thankful to BRNS for financial support.

References

[1] H. Yoneyama, Y. Yamashita, H. Tamura, Nature 282 (1979) 817.
[2] J. Munaz, X. Doménech, J. Appl. Electrochem. 20 (1990) 518.
[3] L.B. Khalil, W.E. Mourad, M.W. Rophael, Appl. Catal. B: Environ. 17 (1998)267.
[4] J. Domenech, J. Munoz, J. Chem. Res. Synopses (1987) 106.
[5] G. Sivalingam, K. Nagaveni, M.S. Hegde, G. Madras, Appl. Catal. B: Environ. 45 (2003) 23.
[6] P. Mohapatra, K.M. Parida, J. Mol. Catal. A: Chem. 258 (2006) 118.
[7] M. Zalas, M. Laniecki, Sol. Energy Mater. Sol. Cells 89 (2005) 287.
[8] Y. Xie, C. Yuan, X. Li, Colloids Surf. A 252 (2005) 87.
[9] X. Yan, J. He, D. Evans, X. Duan, Y. Zhu, Appl. Catal. B: Environ. 55 (2005)243.
[10] H. Cuiying, Y. Wansheng, D. Liqin, L. Zhibin, S. Zhengang, Z. Lancui, Chin. J. Catal. 27 (2006) 203.
[11] T. Peng, D. Zhao, H. Song, C. Yan, J. Mol. Catal. A: Chem. 238 (2005) 119.
[12] Y. Zhang, H. Zhang, Y. Xu, Y. Wang, J. Solid State Chem. 117 (2004) 3490.
[13] F. Li, X. Li, M. Hou, Appl. Catal. B: Environ. 48 (2004) 185.
[14] P. Mohapatra, S.K. Samantaray, K.M. Parida, J. Photochem. Photobiol. A: Chem. 170 (2005) 189.
[15] K.N.P. Kumar, A. Burggraaf, J. Mater. Chem 3 (1993) 141.
[16] R. Gopalan, Y.S. Lin, Ind. Eng. Chem. Res. 34 (1995) 1189.
[17] G. Boschloo, A. Hagfeldt, Chem. Phys. Lett. 370 (2003) 381.
[18] M.S.P. Francisco, V.R. Mastelaro, Chem. Mater. 14 (2002) 2514.
[19] J. Lin, J.C. Yu, J. Photochem. Photobiol. A: Chem. 116 (1998) 63.
[20] D.W. Hwang, J.S. Lee, W. Li, S.H. Oh, J. Phys. Chem. B 107 (2003) 4963.
[21] Y.H. Zhang, H.S. Zhang, Y.X. Xu, Y.G. Wang, J. Mater. Chem. 13 (2003) 2261.
[22] H. Zollinger, Color Chemistry: Synthesis Properties and Applications of Organics Dyes and Pigments, 2nd revised ed., VCH, Weinheim, 1991.
[23] C. Galindo, P. Jacques, A. Dalt, Chemosphere 45 (2001) 997.
[24] G. Soler-Illia, A. Louis, C. Sanchez, Chem. Mater. 14 (2002) 750.
[25] J. Yu, L. Zhang, Z. Zheng, J. Zhao, Chem. Mater. 15 (2003) 2280.

[26] K. Karakitsou, X. Verykios, J. Phys. Chem. 97 (1993) 1184.
[27] S.T. Martin, C.L. Morrison, M.R. Hoffmann, J. Phys. Chem. 98 (1994) 13695.
[28] A. Mills, S. Morris, R. Davies, J. Photochem. Photobiol. A: Chem. 70 (1993)183.
[29] K.T. Ranjit, I. Willner, S.H. Bossmann, A.M. Braun, Environ. Sci. Technol. 35 (2001) 1544.
[30] An-Wu Xu, Yuan Gao, Han-Qin Liu, J. Catal. 207 (2002) 151.
[31] M.R. Hoffmann, S.T. Martin, W. Chio, D.W. Bahnemann, Chem. Rev. 95 (1995) 69.
[32] G.M. Liu, J.C. Zhao, New J. Chem. 24 (2000) 411.
[33] M. Chio, M.R. Hoffmann, J. Phys. Chem. 100 (1996) 2161.